Chemical Engineering Journal 346 (2018) 289–297

Contents lists available at ScienceDirect

Chemical Engineering Journal

journal homepage: www.elsevier.com/locate/cej

Chemically and thermally stable isocyanate microcapsules having good self-healing and self-lubricating performances

Dawei Sun[a,b], Yong Bing Chong[c], Ke Chen[c], Jinglei Yang[a,*]

[a] Department of Mechanical and Aerospace Engineering, Hong Kong University of Science and Technology, Hong Kong Special Administrative Region
[b] Beijing University of Technology, College of Materials Science and Engineering, Beijing 100124, China
[c] School of Mechanical and Aerospace Engineering, Nanyang Technological University, Singapore

HIGHLIGHTS

- The double-layered shell was successfully formed around HMDI droplets.
- The final shell is robust against attacks from heat, water and organic solvents.
- Final smart coatings present good self-healing and self-lubricating behaviors.

GRAPHICAL ABSTRACT

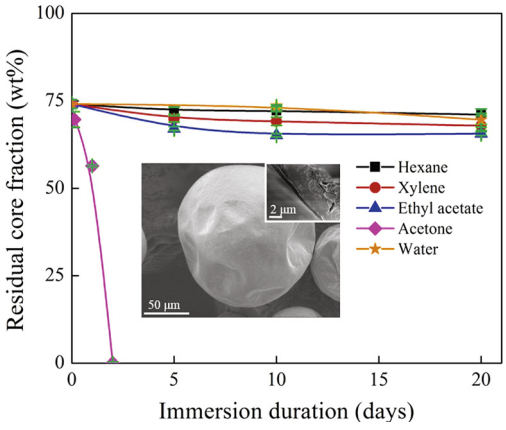

ARTICLE INFO

Keywords:
Microcapsules
Organic solvents resistance
Water resistance
Double-layered shell
Self-healing
Self-lubricating

ABSTRACT

A new approach was developed to load 4,4′-bis-methylene cyclohexane diisocyanate in microcapsules, with outstanding stability in thermal and chemical environments, and excellent efficiency for both self-healing and self-lubricating uses. Well-dispersed microcapsules with diameter of 80 ± 22 μm and shell thickness of 3.8 ± 0.2 μm were produced with a core fraction of 74 ± 1.3 wt% as determined by titration. In thermal environments, the microcapsules started to lose 5% mass at 230 °C, which was higher than the boiling point of pure HMDI and thermal decomposition temperature of shell material. In chemical environments (hexane, xylene, ethyl acetate and water), the impermeable microcapsules reserved more than 90% of original core material after 20 days immersion. More interestingly, final microcapsules survived successfully in acetone losing only 25% of core material after 24 h. Parameters including microcapsules size, concentrations, immersion durations and solvent polarity were investigated systematically to obtain the stability of microcapsules in organic solvents. The smart coatings (10 wt% microcapsules) showed outstanding self-healing anticorrosion efficiency in sodium chloride solutions, and their friction coefficient decreased by 80% than control samples.

* Corresponding author.
E-mail address: maeyang@ust.hk (J. Yang).

https://doi.org/10.1016/j.cej.2018.04.046
Received 12 December 2017; Received in revised form 4 April 2018; Accepted 7 April 2018
Available online 07 April 2018
1385-8947/

1. Introduction

Evolving from self-healing composites [1], self-healing coatings are of particular interest due to their intellectualization and efficiency in steel anticorrosion application [2–6]. Self-healing anticorrosion performances were normally realized through embedded microcapsules, which in broken cases released automatically healing agents into crack areas to recover the protective life of coatings [1–2]. Traditional double-component healing chemistry required different active agents to meet stoichiometrically at damaged areas for satisfying performances [2], while this process was uncontrollable practically. Here proposed timely more viable one-component healing chemistry, where the cure of healing agents was initiated by surrounding light [7,8], moisture [9–11] or oxygen [12–14]. Among all one-component healing agents, water reactive isocyanates drew extensive attentions due to easy operation and great anticorrosion performances.

When isocyanates as healing agents were applied in anticorrosion coatings, the impermeability of microcapsules in both water and organic solvents was urgently concerned. Microcapsules shells were normally fabricated through interfacial [2,10,15,16] or in situ [17–19] protocols, accompanied by introducing inorganic fillers [14,20–22], boosting crosslink density [23,24], and multi-layered structures [25–27] to improve robustness. Wu et al. developed hybrid shells [22] and highly cross-linked PUF shells [24] to load hexamethylene diisocyanate (HDI) with longer lifetime of microcapsules in organic solvents. Sun et al. [25] encased HDI through double-layered polyurea shells for better stability in organic solvents. Yi et al. [28] synthesized hybrid shell-layers through Pickering emulsion, and final microcapsules (isophorone diisocyanate as core) showed exceptional stability in water. Sun et al. [29] applied double-layered PUF/Polyurea shells to boost the service life of encapsulated 4,4′-bis-methylene cyclohexane diisocyanate (HMDI) in water. Nguyen et al. [30] load HDI within hydrophobic microcapsules showing stable core fraction in water for 1 day. Li et al. [31] applied thioether microcapsules to encase isophorone diisocyanate (IPDI), and final core contents dropped by 18% after 7 days in water. However, microcapsules surviving long-termly in both organic solvent and water are still in a high demand.

Besides self-healing, self-lubricating function of coatings was another promising application through the introduction of microcapsules [32,33]. Khun et al. [32] used liquid wax as core material of microcapsules to improve the self-lubricating performance of epoxy coatings. Bandeira et al. [34] introduced polysulphone microcapsules containing ion liquid in coatings with lower friction coefficient. Based on the similar mechanism, such lubricants as lubricant oil [35], tung oil [36], oleylamine [37], and methyl silicone oil [38] were also encapsulated and applied to self-lubricating composites. However, there is a lack of smart coatings with both self-healing and self-lubricating performances. HDI-filled microcapsules were studied tentatively to retard abrasion without satisfying performances, presumably resulted from low core fraction of microcapsules [33].

Herein, we encapsulated HMDI through double-layered shells to improve the stability of microcapsules in both water and organic solvents. The inner-layered polyurea shell was prepared from interfacial polymerization between TEPA and isocyanates, while the outer-layered PUF shells were prepared by polymerizing PUF prepolymer in acidic environments. The stability of microcapsules was characterized by residual core fractions and morphologies after being immersed in water or organic solvents. Finally, the microcapsules were dispersed in epoxy coatings to observe the self-healing and self-lubricating performances.

2. Experimental sections

2.1. Materials

4,4-Diphenylmethane diisocyanate prepolymer (Suprasec 2644) was obtained from Huntsman. HMDI, tetraethylenepentamine (TEPA), gum Arabic, formaldehyde aqueous solution (35–37 wt%), urea, resorcinol, ethylene maleic anhydride (EMA), hydrogen chloride (HCl, 0.1 M), sodium hydroxide (NaOH), sodium chloride (NaCl), hexane, xylene, ethyl acetate and acetone were purchased from Sigma-Aldrich. Epolam 5015 and hardener 5014 were purchased from Axson. All chemicals in this investigation were used as received without further purification.

2.2. Synthesis of microcapsules

The synthesis of final microcapsules was divided into two steps. Polyurea shells were firstly synthesized through interfacial reaction (**IL-microcapsules**), followed by covering a layer of poly-urea-formaldehyde resin (PUF) shell via in situ polymerization (**DL-microcapsules**).

1.5 g of Suprasec 2644 was dissolved uniformly into 13.5 g of HMDI as oil phase, which was then emulsified into micro-droplets in 90 mL of gum Arabic aqueous solutions (2.5 wt%) at 30 °C under mechanical agitation of 650 RPM. The emulsion was stabilized for 45 min. Subsequently, 54 g of TEPA aqueous solution (30 wt%) was slowly added and system temperature was raised to 65 °C. After 60 min, the IL-microcapsules slurry was decanted and rinsed with deionized (DI) water for 4–5 times for following operations.

To prepare PUF shells, urea-formaldehyde (UF) prepolymer was firstly synthesized by reacting 18.99 g of formaldehyde aqueous solutions with 7.5 g of urea under pH value of 7.5–8.5 at temperature of 70 °C for 1 h. Then, the UF prepolymer, 4.5 g of resorcinol and 180 mL of EMA aqueous solutions (1.25 wt%) were mixed well with the IL-microcapsules slurry, and the pH value of mixture was adjusted to 3.0. After 50 min at room temperature under agitation rate of 200 RPM, the system was heat to 55 °C for 2 h. Finally, the suspension of DL-microcapsules was rinsed with DI water for several times, and then dried in air for 12 h for future characterizations.

Under agitation rate of 450 RPM, 650 RPM and 850 RPM during emulsification process, the diameters of corresponding microcapsules were 158 ± 42 μm, 80 ± 22 μm, and 59 ± 17 μm, respectively. Unless otherwise specified, typical microcapsules used in this study have diameter of 80 ± 22 μm.

2.3. Characterizations of microcapsules

The morphologies of microcapsules were observed through field emission scanning electron microscope (FESEM, Joel, Model: JSM-7600F) based on Au sputter-coated samples. Microcapsules were scattered on conductive tape, and some of them were chopped with razor blade to facilitate observation of cross section profiles.

Nuclear magnetic resonance (NMR) was used to analyze the chemical composition of core material. The specification of NMR was 400 MHz spectrometers (Bruker AV400MHz, QNP probe) and the residual solvent peak was used as an internal reference: proton (chloroform δ 7.26).

2.4. Core fraction and thermal stability

To obtain the core fraction, certain mass of microcapsules was crushed completely followed by being flushed into a glass beaker with much acetone. The core fraction of microcapsules was obtained from titration according to ASTM D2572-97 based on the following Eqs. (1) and (2):

$$m_{(HMDI)} = 262.35 \times \frac{1}{2} \times n_{NCO} = 262.35 \times \frac{(V_{(blank)} - V) \times c_{(HCl)}}{2000} \quad (1)$$

$$\text{Core fraction (wt\%)} = \frac{m_{(HMDI)}}{m_{(microcapsules)}} \times 100\% \quad (2)$$

where $m_{(HMDI)}$ (g) is the mass of HMDI core. 262.35 is the equivalent

mass of HMDI. $V_{(blank)}$ (mL) and V (mL) are the volumes of the standard HCl (0.1 M) aqueous solution consumed by blank samples and titration samples, respectively. $c_{(HCl)}$ is the normality of standard HCl (0.1 M) aqueous solution, core fraction (wt%) is the core fraction of microcapsules, and $m_{(microcapsules)}$ (g) is the mass of sample.

The thermal stability of microcapsules was characterized through thermogravimetric analysis (TGA). Unless otherwise indicated, a heating rate of 10 °C min^{-1} in nitrogen atmosphere was applied. 10–20 mg of typical microcapsules, broken microcapsules, shell material and pure HMDI was heat gradually from room temperature to 600 °C. The temperature at 5 wt% mass loss was set as the beginning mass loss temperature of samples.

2.5. Permeability of different shell layer

In order to study the permeability of polyurea and PUF shells, both IL-microcapsules and DL-microcapsules were stored in ambient water for 20 days and in hexane for 5 days at a concentration of 5 wt%, respectively, and characterized in terms of morphologies and residual core fractions.

2.6. The stability of microcapsules in chemical environments

The stability of microcapsules in chemical environments was characterized by residual core fractions and morphologies after periodic intervals in organic solvents or water.

2.6.1. The stability of microcapsules in water

The stability of microcapsules in water was measured by storing typical ones in ambient water at a concentration of 5 wt% for 10 days and 20 days, respectively.

2.6.2. The stability of microcapsules in organic solvents

2.6.2.1. The investigation of immersion durations and solvents polarity. Typical microcapsules were exposed in ambient hexane (Polarity: 0), xylene (Polarity: 1.4) and ethyl acetate (Polarity: 5.3) at a concentration of 5 wt% for 5 days, 10 days, and 20 days, respectively. In acetone (Polarity: 10.4), the immersion durations were 3 h, 24 h and 48 h, respectively.

2.6.2.2. The investigation of microcapsule size. Microcapsules with different diameters (158 ± 42 μm, 80 ± 22 μm, 59 ± 17 μm) were immersed in ambient ethyl acetate for 5 days at a concentration of 5 wt %.

2.6.2.3. The influence of microcapsules concentration. Typical microcapsules were soaked in ethyl acetate at different concentrations (2.5 wt%, 5 wt% and 10 wt%) for 5 days.

2.7. The characterization of smart coatings

The characterization of smart coatings contained self-healing and self-lubricating tests, and control samples without microcapsules were fabricated for comparison. Smart coatings were prepared by dispersing uniformly 10 wt% conditioned microcapsules in pure epoxy resin, which was prepared by formulating Epolam 5015 and hardener 5014 at recommended mass ratio of 3:1, followed by degassing under vacuum for 20 min. Fresh microcapsules were stored in ambient ethyl acetate for 5 days to obtain conditioned microcapsules after dry.

2.7.1. The test of self-healing samples

Self-healing samples were fabricated by covering smart coating on steel panels (50 × 50 × 2 mm^3), which had been polished through sand paper, and then washed by water and acetone to remove surficial impurities. The coating thickness was adjusted within 300–400 μm after cure. After ambient cure for 24 h, first batch of scratches (Labeled as No. 1) were created by razor blades. Samples were then soaked in NaCl (1 M) aqueous solutions for 20 days. Subsequently, the second batch of damages (Labeled as No. 2) was scribed manually at blank places of the same samples, followed by immersion in NaCl solutions for another 24 h. The morphologies of scratches were imaged through FESEM.

In addition, the electrochemical testing was used to observe the occurrence of self-healing process. Firstly, the self-healing samples were stored in NaCl aqueous solutions (1 M) for 20 days before manual scribing. Subsequently, the scratched samples were tested by EIS experiments (Gamry Reference 600 potentiostat) in NaCl aqueous solutions (1 M) as electrolyte solutions. In detail, the swept frequency and AC amplitude was set as 10^{-2}–10^{5} and 20 mV, respectively.

2.7.2. The test of self-lubricating samples

Tribological test was applied to analyze self-lubricating properties of samples, which were prepared by adding resins in a PTFE cylindrical mold with diameters of 30 mm. After cure for 24 h at room temperature, the surfaces of samples were rubbed down with 4000 mesh sand paper and then flushed with water and ethanol prior to tribological test.

Tribological tests were conducted by rolling a steel ball (Cr6, 6 mm in diameter) on sample surfaces through a ball-on-disc micro-tribometer (CSM), and the diameter of circular wear track was set as 3 mm. The experimental parameters were shown in the following: load: 3 N; velocity: 5 cm/s; wear laps: 50,000 laps. The friction coefficient, wear width and wear depth of all samples were measured for analysis. Both wear depth and wear width of wear track were obtained through surface profilometry, and results were obtained based on the average value of at least 12 points.

3. Result and discussion

3.1. Formation mechanism of double-layered shell

Microcapsule shells were composed of inner-layered polyurea shells and outer-layered PUF shells. The polyurea shells were synthesized by interfacial polymerization in an oil/water emulsion. TEPA as crosslinker was favorable for the formation of polyurea shells with higher crosslink density than traditional polyurethane shells, since the reactivity of amine/NCO was thousands of times higher than that of polyols/NCO [39]. At the surfaces of micro-droplets, TEPA reacted rapidly with both Suprasec 2644 and HMDI [40], while polyols tended to react with more active Suprasec 2644 producing loose polyurethane shells[9]. However, the high reactivity of amine/NCO brought serious coalescence issues of microcapsules once TEPA was added in emulsions. For well-dispersed microcapsules, the numbers of NCO functional groups at droplets surfaces had to be reduced by extending emulsification durations [29].

PUF shells were prepared by in situ polymerization on the surfaces of polyurea shells. Acidic polymerization of urea-formaldehyde prepolymer boosted the crosslink density of PUF shells [41], and the prepolymer was synthesized by reacting urea and formaldehyde in alkaline environments [42].

3.2. Morphology of microcapsules

Microcapsules morphologies and shell profiles were presented in Fig. 1. Fig. 1a showed well-dispersed microcapsules with mean diameter of 80 ± 22 μm. Every microcapsule had smooth and dense outer surface (Fig. 1b), and hollow inner structure (Fig. 1c). In addition, the cross-sectional shell profile (Fig. 1d) demonstrated obviously double-layered structure. The average shell thickness of microcapsules was 3.8 ± 0.2 μm, consisting of PUF and polyurea shell thickness of 387 ± 40 nm and 3.5 ± 0.2 μm, respectively.

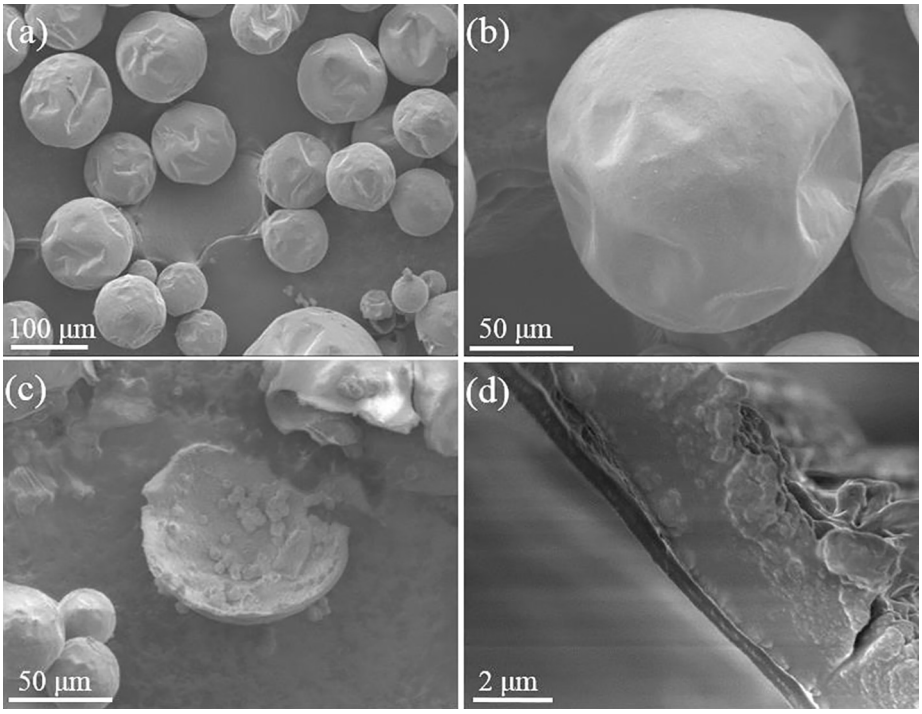

Fig. 1. The morphologies of typical microcapsules: (a) overview of microcapsules with distributed diameters; (b) individual microcapsule with smooth surface; (c) hollow structure of microcapsules with little solid impurities; and (d) detailed information of shell profile.

3.3. Chemical composition of core material

The chemical composition of core material was analyzed by ^{1}H NMR. As shown in Fig. 2, the spectrum of core material (Fig. 2b) was highly similar with that of pure HMDI (Fig. 2a), demonstrating that HMDI was encapsulated successfully.

3.4. Core fraction and thermal stability of microcapsules

The practical core fraction of typical capsules was obtained by titration method, and it (74 ± 1.3 wt%) was nearly equal to theoretical value (73 ± 4.6 wt%). The theoretical core fraction of microcapsules was estimated as following: $\frac{\rho_{HMDI}}{\rho_{polyurea}}\left(\frac{D-2*S}{D}\right)^{3}$, where D was the diameter, and S was the shell thickness of microcapsules. From our SEM images, D was 80 ± 22 μm, and S was 3.8 ± 0.2 μm. ρ_{HMDI} (1.066 g/cm^3) and $\rho_{polyurea}$ (1.066 g/cm^3) were the density of HMDI and regular

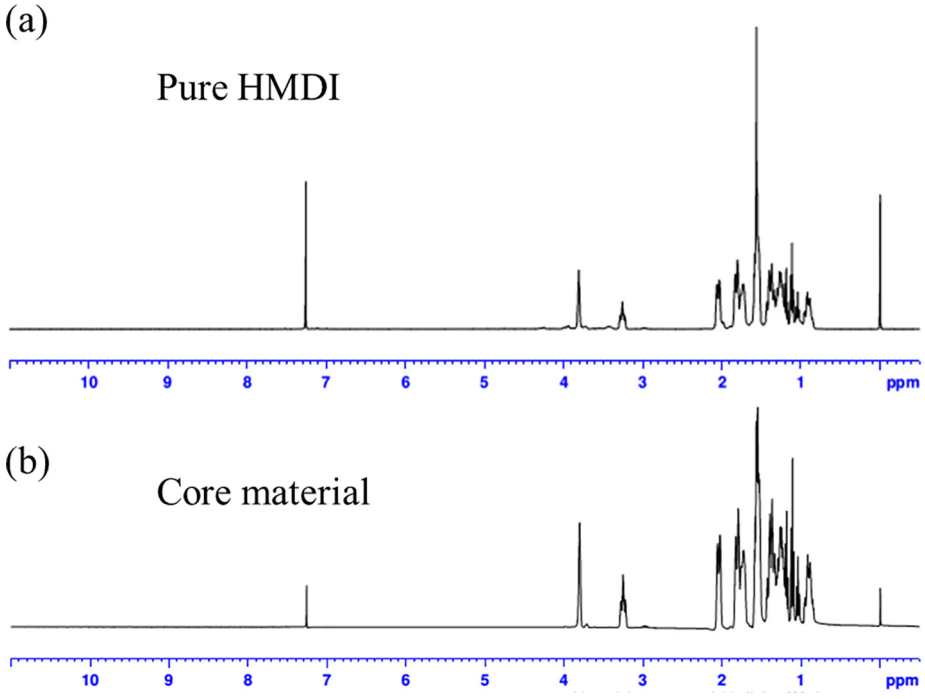

Fig. 2. Comparisons of ^{1}H NMR spectras of core material with that of pure HMDI.

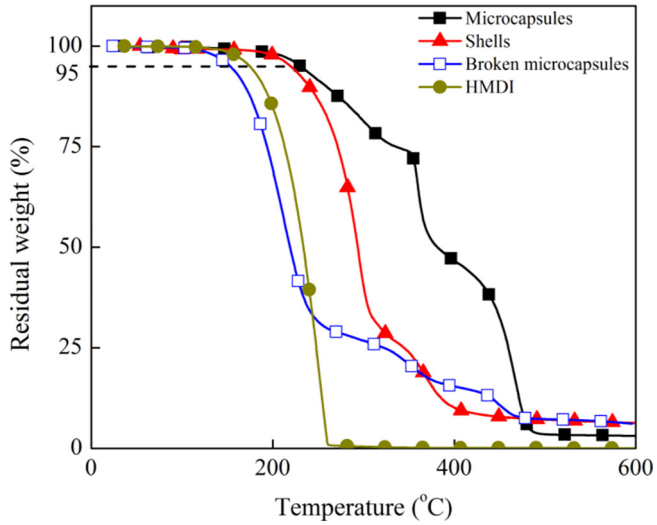

Fig. 3. TGA curves of typical microcapsules, shell materials, pure HMDI, and broken microcapsules when system temperature was raised from room temperature to 600 °C at a rate of 10 °C min^{-1} in N_2 atmosphere.

polyurea material, respectively.

The thermal stability of microcapsules was assessed by TGA. The mass loss curves of all materials were plotted in Fig. 3 as a function of temperature. Shell material lost mass of 5 wt% at 220 °C (beginning mass loss temperatures) and finished decomposition by 600 °C leaving approximate 7.2 wt% residue. The beginning mass loss temperature of other materials was 174 °C (pure HMDI), 230 °C (typical microcapsules), and 153 °C (broken microcapsules), respectively. The highest beginning mass loss temperature indicated excellent thermal stability of final microcapsules, since impermeable shells trapped HMDI vapor under temperature higher than the boiling point (168 °C) of pure HMDI, unless microcapsules were broken. Even when shell material was decomposed by 5 wt% at 220 °C, more than 90% of HMDI core was still reserved. Interestingly, encapsulated isocyanates were firstly reported with such great thermal stability [9,22–25].

3.5. Permeability of different shell layers

The permeability of polyurea and PUF shells was evaluated through the stability of IL-microcapsules and DL-microcapsules in water and hexane, respectively.

IL-microcapsules and DL-microcapsules were soaked in ambient water for 20 days to test the water resistance of polyurea shell, respectively. As shown in Fig. 4a and c, both residual microcapsules were hollow without solid impurities. The core fraction of IL-microcapsules decreased from 91.6 ± 0.8 wt% to 73.0 ± 2.2 wt% after immersion, and that of DL-microcapsules dropped from 74.1 ± 1.3 wt% to 69.6 ± 3.1 wt%. The impermeable polyurea shells allowed little water diffusion-in microcapsules resulting in hollow structure and minor decrease of core fraction. For comparison, the encapsulated HDI was depleted completely after 48 h in ambient water [9].

In addition, both microcapsules were stored in hexane for 5 days to assess the organic solvents resistance of PUF shells. As shown in Fig. 4b, IL-microcapsules collapsed completely into debris because all HMDI core was extracted out. However, DL-microcapsules remained well spherical (Fig. 4d) with marginal decrease of core fraction from 74.1 ± 1.3 wt% to 72.2 ± 1.0 wt% because PUF shells contributed the good stability of final microcapsules in organic solvents.

Therefore, it was reasonable to conclude that polyurea and PUF shells provided final microcapsules outstanding stability in water and organic solvents, respectively.

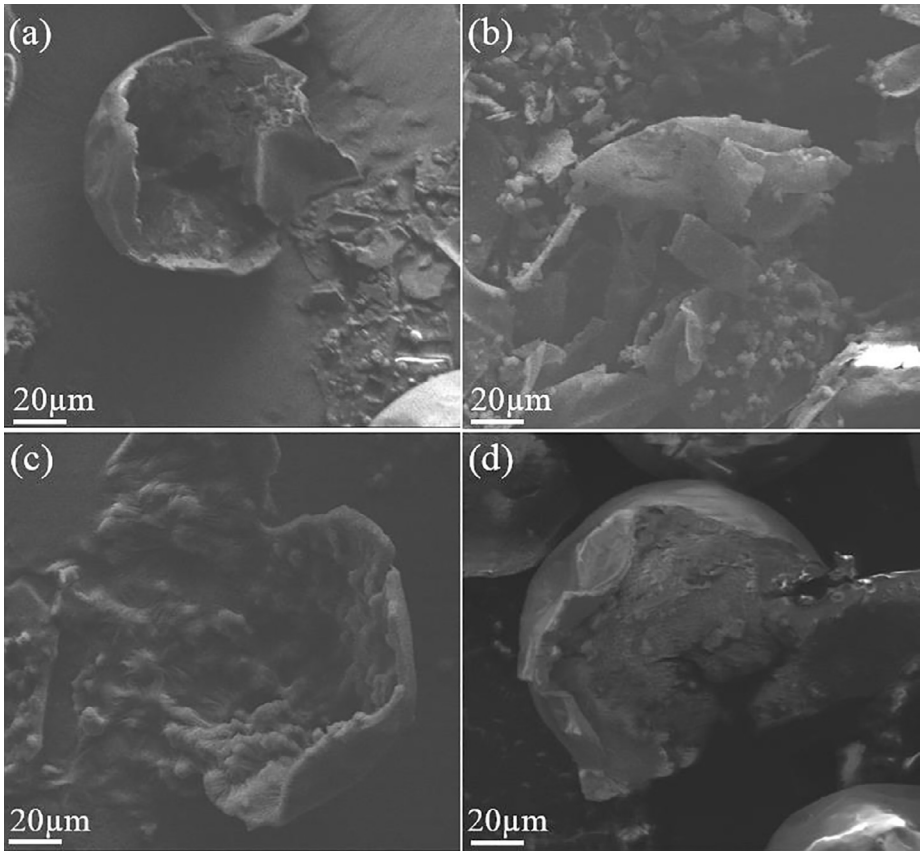

Fig. 4. The permeability of polyurea and PUF shells was analyzed by testing the stability of IL-microcapsules and DL-microcapsules in water or hexane, respectively. (a) The hollow structure of IL-microcapsules in water; (b) Collapsed IL-microcapsules in hexane. (c) The hollow structure of DL-microcapsules in water; and (d) Spherical DL-microcapsules in hexane.

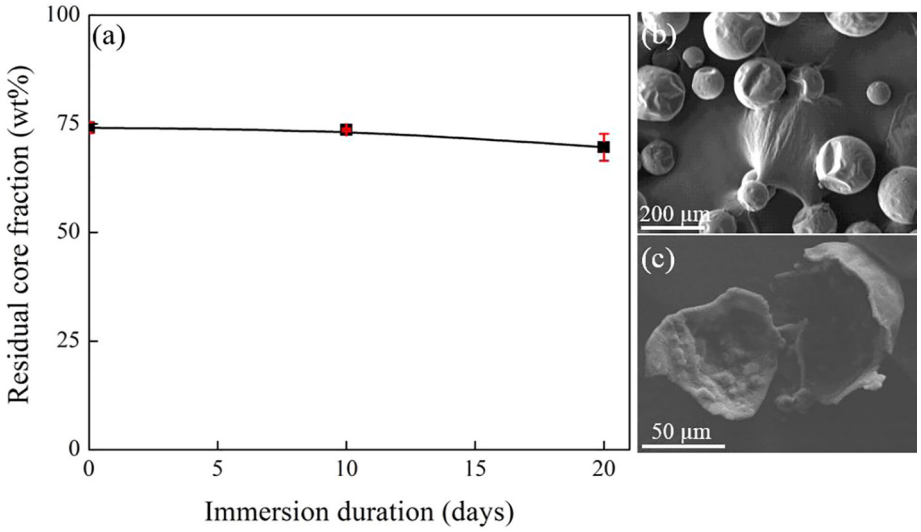

Fig. 5. The water resistance were tested by immersing typical microcapsules in water for different durations. (a) The residual core fraction of microcapsules was plotted as a function of immersion durations. (b and c) The outer and inner morphologies of residual microcapsules after 20 days in ambient water, respectively.

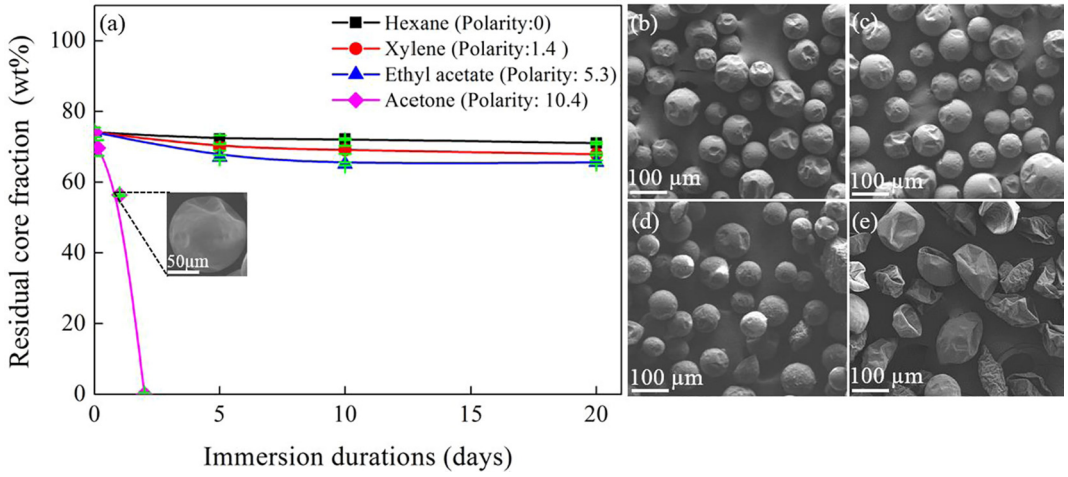

Fig. 6. The organic solvents resistance was measured by immersing microcapsules in different organic solvents for different durations. (a) The residual core fractions of microcapsules was plotted as a function of immersion durations. (b–d) The morphologies of residual microcapsules after immersion in hexane, xylene, and ethyl acetate for 20 days, respectively. (Inset of a, e) The morphologies of microcapsules after being immersed in acetone for 24 h and 48 h, respectively.

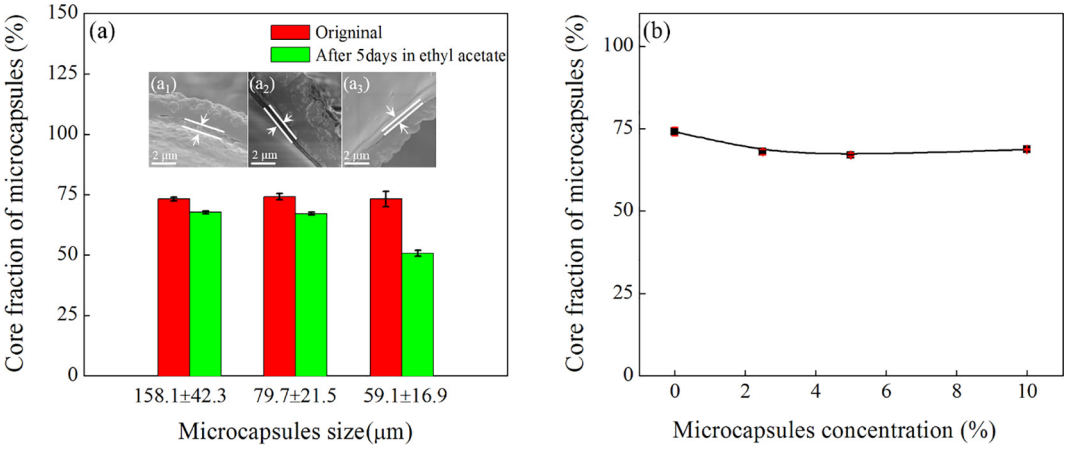

Fig. 7. The influence of size and concentrations on organic solvents resistance of microcapsules. (a) The core fraction of microcapsules with different diameters before and after immersion in ethyl acetate. (a_1, a_2 and a_3) The PUF shell thickness of microcapsules with different diameters. (b) The residual core fraction of typical microcapsules as a function of microcapsule concentrations in ethyl acetate.

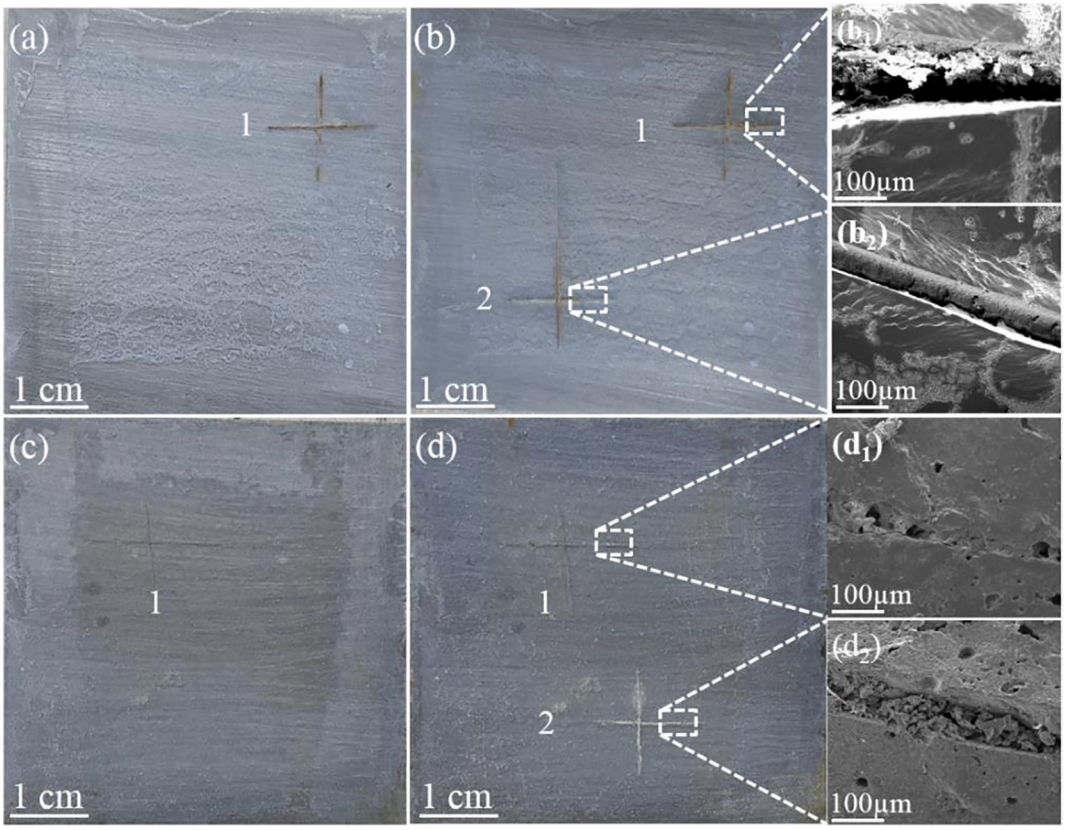

Fig. 8. (a, b) Corrosion performance of pure epoxy coatings with No. 1 and No. 2 scratches, respectively; (b_1 and b_2) The view within scratches No. 1 and No. 2 of pure epoxy coatings, respectively; (c, d) The anticorrosion performance of smart coatings with No. 1 scratches and No. 2 scratches, respectively. (d_1 and d_2) The view within scratches No. 1 and No. 2 of smart coatings, respectively.

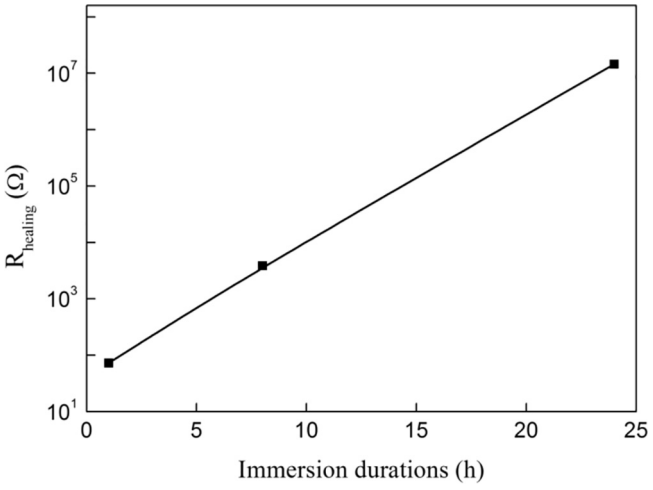

Fig. 9. The resistance ($R_{healing}$) of self-healing samples was ploted as a function of immersion duration in 1 M NaCl solution.

3.6. The stability of microcapsules in chemical environments

3.6.1. Stability of microcapsules in water

The stability of microcapsules in water had to be considered when isocyanates were encapsulated for anticorrosion applications in humid environments. The typical microcapsules were immersed in ambient water for different durations to test their water resistance. The residual core fraction of microcapsules was plotted in Fig. 5 as a function of immersion durations. When immersion duration was extended from 0 day to 10 days and 20 days, the core fraction of microcapsules decreased from 74.1 ± 1.3 wt% to 73.6 ± 1.3 wt% and 69.6 ± 3.1 wt%, respectively. Although slight reduction of core fraction was observed due to the consumption of HMDI core by surrounding water molecules, more than 90% of original core material was still reserved after 20 days. Moreover, the morphology of residual microcapsules was also similar with the fresh showing smooth outer surface (Fig. 5b) and hollow inner structure (Fig. 5c). The outstanding stability of microcapsules in water was mainly resulted by impermeable inner–layered polyurea shells to isolate surrounding water molecules.

3.6.2. Stability of microcapsules in organic solvents

In commercial coatings, organic solvents were usually applied to assist easy operation, requiring good stability of embedded microcapsules. Microcapsules with a range of diameters were soaked in various organic solvents at different concentrations for designed durations, respectively, and then characterized by residual core fractions and morphologies. Many parameters were investigated including immersion durations, solvent polarity, microcapsules size and concentrations.

3.6.2.1. Immersion durations and solvent polarity. To study the influence of immersion duration and solvent polarity on the stability of microcapsules, typical microcapsules were immersed in hexane, xylene, ethyl acetate and acetone for different durations. The residual core fraction of microcapsules was plotted in Fig. 6 as a function of immersion durations. In hexane, xylene and ethyl acetate, the core material was extracted slowly out with immersion durations until 5 days, followed by a stable plateau due to osmotic balance, in agreement with previous publications [25]. Besides, solvent polarity also affected microcapsules stability. In more polar solvents (hexane < xylene < ethyl acetate < acetone), the loss of core

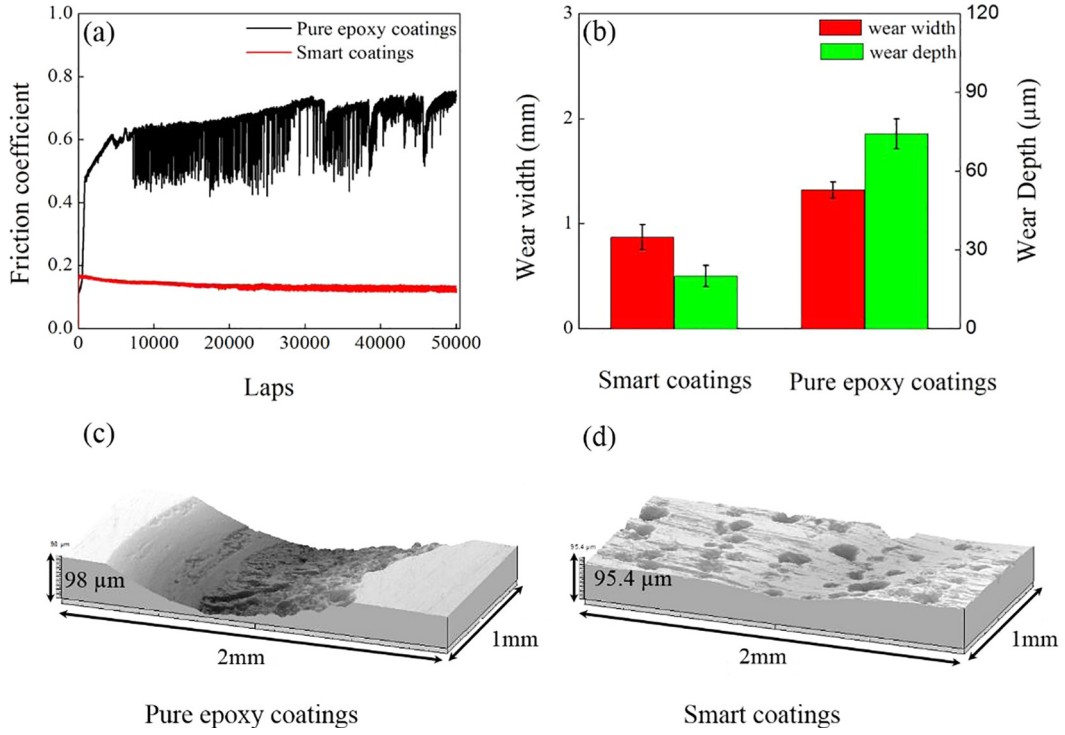

Fig. 10. Self-lubricating performance of pure epoxy coatings and smart coatings. (a) The friction coefficients of both coatings varied as a function of wear laps. (b) Wear width and depth of both coatings. The topographies of samples after tribological tests were shown in (c) pure epoxy coatings and (d) smart coatings.

material was more and faster, because the polymeric shells appeared to be swelled more seriously, resulting in larger mesh size and hence more release of liquid core [25].

Although a little leakage occurred, microcapsules still reserved massive core material and remained stable morphologies in organic solvents. When immersion duration was 20 days, the residual core fractions of microcapsules was 71.1 ± 0.3 wt% in hexane, 67.9 ± 0.7 wt% in xylene, and 65.6 ± 0.5 wt% in ethyl acetate, respectively. Additionally, all microcapsules appeared well spherical, as shown in Fig. 6b (hexane), c(xylene), and d (ethyl acetate). Even in acetone for 24 h, microcapsules still reserved 56.4 ± 0.4 wt% core fraction and spherical shape (inset of Fig. 6a). Unfortunately, all core material was extracted out after 48 h (Fig. 6a), along with serious shrinkage of microcapsules (Fig. 6e). Comparing with complete leakage of traditional microcapsules in acetones within 1 h [24,25], our microcapsules were more applicable in harsh conditions.

3.6.2.2. Microcapsules size and concentration. Microcapsules with different diameters were immersed in ethyl acetate for 5 days to study the influence of microcapsules size on final stability. As shown in Fig. 7a, the core fraction of residual microcapsules with diameters of 158 ± 42 μm, 80 ± 22 μm and 60 ± 17 μm decreased by 7.5%, 9.6%, and 30.7%, corresponding to the PUF shell thickness of 422 ± 36 nm (Fig. 7a$_1$), 387 ± 40 nm (Fig. 7a$_2$), and 309 ± 27 nm (Fig. 7a$_3$), respectively. Smaller microcapsules had larger specific interface area, resulting in the formation of thinner shell layer from in situ polymerization. Therefore, more leakage occurred to smaller microcapsules due to their thinner PUF shells and worse resistance to organic solvents.

The influence of concentrations on microcapsules stability was investigated by immersing typical microcapsules in ethyl acetate at different concentrations. In Fig. 7b, the residual core fraction was 68.0 ± 0.8 wt%, 67.0 ± 0.6 wt% and 68.7 ± 0.1 wt% corresponding to microcapsules concentrations of 2.5 wt%, 5 wt% and 10 wt%, respectively. Nearly stable core fraction implied little influence of concentration on microcapsules stability in organic solvents.

4. Characterization of smart coatings

Although microcapsules had wide applications in self-healing [3] and self-lubricating materials [33], bi-functional smart coatings still remained undeveloped. Herein, new smart coatings were fabricated successfully and showed outstanding self-healing and self-lubricating performances.

4.1. Self-healing test of smart coatings

Self-healing test of smart coatings was shown in Fig. 8. Severe corrosion occurred to control samples (Fig. 8a(No. 1)) after 20 days immersion in salty water due to the direct exposure of steel substrates in corrosive environments (Fig. 8b$_1$). In dramatic contrast, the smart coatings presented no visible corrosion evidence, as shown in Fig. 8c (No. 1), because the released HMDI from broken microcapsules polymerized with moisture to seal the scratches (Fig. 8d$_1$).

Even after long-term storage (20 days) in water, smart coatings still remained active. The No.2 scratches were sealed completely (Fig. 8d$_2$) and free of rust (Fig. 8d). However, serious rust (Fig. 8b(No. 2)) occurred to control samples because of empty scratches (Fig. 8b$_2$). Furthermore, EIS experiments provided further evidence of self-healing process. As shown in Fig. 9, the self-healing process was accompanied with the increase of coating resistance, which was raised greatly from 72.5 Ω to 1.5 × 10^7 Ω when immersion durations were extended from 1 h to 24 h, in agreement with previous publications [29,43].

4.2. Self-lubricating test of smart coatings

The self-lubricating results of smart coatings were presented in Fig. 10. Fig. 10a showed the friction coefficient of samples as a function of wear laps. As proceeding with friction process, the friction coefficient of smart coating decreased obviously with wear laps due to the release of more HMDI, while that of pure epoxy samples kept increasing resulted by larger contact interface and then more serious mechanical interlock. The microcapsules debris was observed clearly on the wear

track of smart coatings, as shown in Fig. 10d. The average friction coefficient of smart coatings was 0.136, while that of control samples was 0.644. The friction coefficient of smart coatings was decreased by 78.9% because of the great lubricating action of HMDI. In previous investigation, weak self-lubricating effects was observed when smart coatings were prepared from encapsulated HDI [33].

The wear loss of samples was characterized by wear width and wear depth, both which were obtained from the profile of wear track based on at least 10 points, as shown in Fig. 10b. The wear width and wear depth of smart coatings were 0.9 ± 0.1 mm and 20.0 ± 4.1 μm, and those of control samples were 1.3 ± 0.1 mm and 74 ± 36 μm, respectively. Obviously, embedding final microcapsules improved obviously the wear loss of epoxy matrix.

Therefore, it was noted that the introduction of encapsulated isocyanates could efficiently improve the self-lubricating performance of epoxy resin.

5. Conclusions

Liquid HMDI were loaded successfully within impermeable double-layered shells. The inner-layered polyurea and outer-layered PUF shells provided microcapsules great stability in water and organic solvents, respectively. Bigger microcapsules survived longer duration in organic solvents with lower polarities. However, immersion concentrations affected slightly the stability of microcapsules. Even after 20 days in water, final microcapsules still remained active for self-healing uses. Besides, the lubricating performances of final microcapsules were also very attractive. In future, the shell strength of microcapsules needs to be further improved. It is more promising to fabricate smaller microcapsules with such good properties.

Acknowledgement

The authors would like to thank the financial support from the Hong Kong University of Science and Technology (Grant#: R9365) of Hong Kong SAR.

References

[1] S.R. White, N. Sottos, P. Geubelle, J. Moore, M.R. Kessler, S. Sriram, E. Brown, S. Viswanathan, Autonomic healing of polymer composites, Nature 409 (2001) 794–797.
[2] S.H. Cho, S.R. White, P.V. Braun, Self-healing polymer coatings, Adv. Mater. 21 (2009) 645–649.
[3] D.G. Shchukin, D. Borisova, H. Möhwald, Self-Healing Polymers: From Principles to Applications, (2013).
[4] M. Samadzadeh, S.H. Boura, M. Peikari, S. Kasiriha, A. Ashrafi, A review on self-healing coatings based on micro/nanocapsules, Prog. Org. Coat. 68 (2010) 159–164.
[5] Y. Yang, M.W. Urban, Self-healing polymeric materials, Chem. Soc. Rev. 42 (2013) 7446–7467.
[6] H.G. Wei, Y.R. Wang, J. Guo, N.Z. Shen, D.W. Jiang, X. Zhang, X.R. Yan, J.H. Zhu, Q. Wang, L. Shao, H.F. Lin, S.Y. Wei, Z.H. Guo, Advanced micro/nanocapsules for self-healing smart anticorrosion coatings, J. Mater. Chem. A 3 (2015) 469–480.
[7] Y.K. Song, C.M. Chung, Repeatable self-healing of a microcapsule-type protective coating, Polym. Chem. 4 (2013) 4940–4947.
[8] D. Zhao, M.Z. Wang, Q.C. Wu, X. Zhou, X.W. Ge, Microencapsulation of UV-curable self-healing agent for smart anticorrosive coating, Chin. J. Chem. Phys. 27 (2014) 607–615.
[9] M. Huang, J. Yang, Facile microencapsulation of HDI for self-healing anticorrosion coatings, J. Mater. Chem. 21 (2011) 11123–11130.
[10] J.L. Yang, M.W. Keller, J.S. Moore, S.R. White, N.R. Sottos, Microencapsulation of isocyanates for self-healing polymers, Macromolecules 41 (2008) 9650–9655.
[11] S.J. Garcia, H.R. Fischer, P.A. White, J. Mardel, Y. Gonzalez-Garcia, J.M.C. Mol, A.E. Hughes, Self-healing anticorrosive organic coating based on an encapsulated water reactive silyl ester: synthesis and proof of concept, Prog. Org. Coat. 70 (2011) 142–149.
[12] M. Samadzadeh, S.H. Boura, M. Peikari, A. Ashrafi, M. Kasiriha, Tung oil: an autonomous repairing agent for self-healing epoxy coatings, Prog. Org. Coat. 70 (2011) 383–387.
[13] S.H. Boura, M. Peikari, A. Ashrafi, M. Samadzadeh, Self-healing ability and adhesion strength of capsule embedded coatings-micro and nano sized capsules containing linseed oil, Prog. Org. Coat. 75 (2012) 292–300.
[14] T. Szabo, J. Telegdi, L. Nyikos, Linseed oil-filled microcapsules containing drier and corrosion inhibitor – their effects on self-healing capability of paints, Prog. Org. Coat. 84 (2015) 136–142.
[15] D.A. McIlroy, B.J. Blaiszik, M.M. Caruso, S.R. White, J.S. Moore, N.R. Sottos, Microencapsulation of a reactive liquid-phase amine for self-healing epoxy composites, Macromolecules 43 (2010) 1855–1859.
[16] D.A. McIlroy, B.J. Blaiszik, M.M. Caruso, S.R. White, J.S. Moore, N.R. Sottos, Microencapsulation of a reactive liquid-phase amine for self-healing epoxy composites, Macromolecules 43 (2010) 1855–1859.
[17] E.N. Brown, M.R. Kessler, N.R. Sottos, S.R. White, In situ poly(urea-formaldehyde) microencapsulation of dicyclopentadiene, J. Microencapsul. 20 (2003) 719–730.
[18] R.S. Jadhav, D.G. Hundiwale, P.P. Mahulikar, Synthesis and characterization of phenol–formaldehyde microcapsules containing linseed oil and its use in epoxy for self-healing and anticorrosive coating, J. Appl. Polym. Sci. 119 (2011) 2911–2916.
[19] L.M. Meng, Y.C. Yuan, M.Z. Rong, M.Q. Zhang, A dual mechanism single-component self-healing strategy for polymers, J. Mater. Chem. 20 (2010) 6030–6038.
[20] M. Li, M.R. Chen, Z.S. Wu, Enhancement in thermal property and mechanical property of phase change microcapsule with modified carbon nanotube, Appl. Energy 127 (2014) 166–171.
[21] M.W. Patchan, B.W. Fuller, L.M. Baird, P.K. Gong, E.C. Walter, B.J. Vidmar, I. Kyei, Z. Xia, J.J. Benkoski, Robust composite-shell microcapsules via pickering emulsification, ACS Appl. Mater. Interfaces 7 (2015) 7315–7323.
[22] G. Wu, J. An, D. Sun, X. Tang, Y. Xiang, J. Yang, Robust microcapsules with polyurea/silica hybrid shell for one-part self-healing anticorrosion coatings, J. Mater. Chem. A 2 (2014) 11614–11620.
[23] P.D. Tatiya, R.K. Hedaoo, P.P. Mahulikar, V.V. Gite, Novel polyurea microcapsules using dendritic functional monomer: synthesis, characterization, and its use in self-healing and anticorrosive polyurethane coatings, Ind. Eng. Chem. Res. 52 (2013) 1562–1570.
[24] G. Wu, J. An, X.Z. Tang, Y. Xiang, J. Yang, A Versatile approach towards multifunctional robust microcapsules with tunable, restorable, and solvent-proof superhydrophobicity for self-healing and self-cleaning coatings, Adv. Funct. Mater. 24 (2014) 6751–6761.
[25] D. Sun, J. An, G. Wu, J. Yang, Double-layered reactive microcapsules with excellent thermal and non-polar solvents resistance for self-healing coatings, J. Mater. Chem. A 3 (2015) 4435–4444.
[26] S. Kang, M. Baginska, S.R. White, N.R. Sottos, Core-shell polymeric microcapsules with superior thermal and solvent stability, ACS Appl. Mater. Interfaces 7 (2015) 10952–10956.
[27] M.W. Patchan, L.M. Baird, Y.-R. Rhim, E.D. LaBarre, A.J. Maisano, R.M. Deacon, Z. Xia, J.J. Benkoski, Liquid-filled metal microcapsules, ACS Appl. Mater. Interfaces 4 (2012) 2406–2412.
[28] H. Yi, Y. Yang, X. Gu, J. Huang, C. Wang, Multilayer composite microcapsules synthesized by pickering emulsion templates and their application in self-healing coating, J. Mater. Chem. A 3 (2015) 13749–13757.
[29] D. Sun, H. Zhang, X.-Z. Tang, J. Yang, Water resistant reactive microcapsules for self-healing coatings in harsh environments, Polymer 91 (2016) 33–40.
[30] L.T.T. Nguyen, X.K.D. Hillewaere, R.F.A. Teixeira, O. van den Berg, F.E. Du Prez, Efficient microencapsulation of a liquid isocyanate with in situ shell functionalization, Polym. Chem. 6 (2015) 1159–1170.
[31] C.M. Li, J.J. Tan, J.W. Gu, L. Qiao, B.L. Zhang, Q.Y. Zhang, Rapid and efficient synthesis of isocyanate microcapsules via thiol-ene photopolymerization in pickering emulsion and its application in self-healing coating, Compos. Sci. Technol. 123 (2016) 250–258.
[32] N.W. Khun, H. Zhang, J.L. Yang, E. Liu, Tribological performance of silicone composite coatings filled with wax-containing microcapsules, Wear 296 (2012) 575–582.
[33] N.W. Khun, H. Zhang, X.Z. Tang, C.Y. Yue, J.L. Yang, Short carbon fiber-reinforced epoxy tribomaterials self-lubricated by wax containing microcapsules, J. Appl. Mech. Trans. ASME 81 (2014) 7.
[34] P. Bandeira, J. Monteiro, A.M. Baptista, F.D. Magalhaes, Tribological performance of PTFE-based coating modified with microencapsulated HMIM NTf2 ionic liquid, Tribol. Lett. 59 (2015) 15.
[35] H.Y. Li, Q. Wang, M.L. Li, Y.X. Cui, Y.J. Zhu, B.H. Wang, H.Y. Wang, Preparation of high thermal stability polysulfone microcapsules containing lubricant oil and its tribological properties of epoxy composites, J. Microencapsul. 33 (2016) 286–291.
[36] H.Y. Li, Y.X. Cui, H.Y. Wang, Y.J. Zhu, B.H. Wang, Preparation and application of polysulfone microcapsules containing tung oil in self-healing and self-lubricating epoxy coating, Colloid Surf. A: Physicochem. Eng. Asp. 518 (2017) 181–187.
[37] G.L. Zhang, G.X. Xie, L.N. Si, S.Z. Wen, D. Guo, Ultralow friction self-lubricating nanocomposites with mesoporous metal-organic frameworks as smart nanocontainers for lubricants, ACS Appl. Mater. Interfaces 9 (2017) 38146–38152.
[38] B. Mu, X. Li, B.P. Yang, J.F. Cui, X. Wang, J.H. Guo, X.M. Bao, L. Chen, Tribological behaviors of polyurethane composites containing self-lubricating microcapsules and reinforced by short carbon fibers, J. Appl. Polym. Sci. 134 (2017) 10.
[39] R. Herrington, K. Hock, Flexible Polyurethane Foams, Dow Chemical, 1997.
[40] G. Woods, Flexible Polyurethane Foams, Springer, 1982.
[41] I. Updegraff, Amino Resins, (1985).
[42] S.S. Jada, The structure of urea—formaldehyde resins, J. Appl. Polym. Sci. 35 (1988) 1573–1592.
[43] M. Huang, J. Yang, Salt spray and EIS studies on HDI microcapsule-based self-healing anticorrosive coatings, Prog. Org. Coat. 77 (2014) 168–175.